Two-state bright solitons in doped fibers with saturating nonlinearity

Ajit Kumar

Department of Physics, Indian Institute of Technology, Hauz Khas, New Delhi-110016, India

Thomas Kurz and Werner Lauterborn

Drittes Physikalisches Institut, Universität Göttingen, Bürgerstraße 42-44, D-37073 Göttingen, Germany
(Received 17 July 1995)

Fundamental bright soliton solutions are studied numerically in a model for pulse propagation in semiconductor-doped glass fibers with exponential saturation of the nonlinear dielectric function. It is shown that the given model possesses two-state soliton solutions in the sense that for a given set of fiber parameters there exist two soliton solutions with the same pulse width but with different peak amplitudes, i.e., with different peak powers. The stability of these solitons under weak perturbations and the effect of the fiber loss are also investigated. A comparison with earlier results for such solitons is made.

I. INTRODUCTION

For the last two decades optical solitons in fibers have attracted much attention from physicists as well as engineers in connection with their tremendous utility in all-optical communication systems [1–11], optical switching devices [12–14], signal processing, optical computing, etc. Recently, especially after Kaplan's work [15,16] and the subsequent development [14,17–19] of his ideas, there has been increasing interest in multistable solitons in fibers made of composite materials. As shown by Enns and co-workers [17–19], it is possible to have easy switching from one stable state of such solitons to another, which makes multistable solitons attractive and useful in applications for ultrafast switching devices.

Experimental results of the measurements of the nonlinear absorption [20,30] in semiconductor-doped glass (SDG) and other composite materials show that nonlinearity saturates at not too high field intensities. Hence, in modeling pulse propagation in fibers made of such materials, one must use the saturating form of the dielectric function or the nonlinear refractive index. Usually one adds a saturating term for the nonlinear refractive index in place of the cubic term in the nonlinear Schrödinger equation (NLSE) and models the pulse dynamics [22–26]. The other way is to take an appropriate saturating form of the dielectric function and derive the differential equation, governing pulse dynamics, from Maxwell's equations or the equivalent nonlinear wave equation using the standard method of slowly varying envelope approximation (SVEA) and averaging over the cross section of the fiber [5,27]. As discussed by Enns and Rangnekar [17], one can model the system by various forms of nonlinearity in the equation. To the best of our knowledge, besides the steplike nonlinearity, the following saturable forms:

$$\varepsilon_{NL}(|\mathbf{E}|^2) = \varepsilon_2 \frac{|\mathbf{E}|^2}{1 + (|\mathbf{E}|^2/I_S)} \tag{1}$$

and

$$\varepsilon_{NL}(|\mathbf{E}|^2) = I_S \varepsilon_2 [1 - \exp(-|\mathbf{E}|^2/I_S)] \tag{2}$$

of the nonlinear dielectric function ε_{NL} are the most frequently used ones in the literature, where ε_2 is the Kerr coefficient for the dielectric function, and I_S is the intensity at which saturation occurs. One of the authors derived a nonlinear and dispersive partial differential equation [28,29] for the study of pulse propagation in SDG fibers described by the dielectric function given by Eq. (2). In this work we numerically determine the fundamental ($N = 1$) bright soliton solutions in this model, study their properties, and compare our results with those obtained for the model based on the nonlinear refractive index change Δn_{NL} given by [22]

$$\Delta n_{NL} = \frac{n_2 |\mathbf{E}|^2}{1 + (|\mathbf{E}|^2/I_s)}, \tag{3}$$

n_2 being the Kerr coefficient for the refractive index related to ε_2 through the expression $\varepsilon_2 = 2n_0 n_2$.

II. MODEL

Consider pulse propagation in a monomode SDG fiber governed by the following nonlinear wave equation:

$$\nabla^2 \mathbf{E} - \frac{1}{c^2} \frac{\partial^2 \mathbf{D}^L}{\partial t^2} = \frac{1}{c^2} \frac{\partial^2 \mathbf{D}^{NL}}{\partial t^2}, \tag{4}$$

where

$$\mathbf{D}^L = \int_0^\infty \varepsilon(t') \mathbf{E}(\mathbf{x}, t - t') dt', \tag{5}$$

$$\mathbf{D}^{NL} = \varepsilon_2 I_S (1 - \exp[-|\mathbf{E}|^2/I_S]) \mathbf{E} \tag{6}$$

are the linear and nonlinear parts of the electric induction vector $\mathbf{D}$, respectively, ε being the linear permittivity. As is customary, we assume the pulse, propagating along the longitudinal axis x of the fiber, to be supported entirely by the fundamental mode (HE_{11} or LP_{01}), and hence we can represent $\mathbf{E}$ as

$$\mathbf{E}(t,\mathbf{r},x)=\mathbf{e}R(\mathbf{r})A(t,x)\exp[-i(\omega t-\beta_0 x)] ,\qquad (7)$$

where $\mathbf{e}$ is the unit vector in the direction of polarization, $\mathbf{r}$ is a vector in the transverse plane (y,z), $R(\mathbf{r})$ is the modal function describing the transverse distribution of the electric field in the mode, $A(t,x)$ is the slowly varying complex envelope amplitude, and β_0 is the propagation constant. Assuming the Gaussian form for transverse intensity distribution and small temporal dispersion, we use the standard procedure based on SVEA and average over the cross section of the fiber [5,27] to obtain from Eqs. (4)–(7) the following nonlinear partial differential equation for the complex envelope amplitude $A(x,t)$:

$$i\left[A_x+\frac{1}{v_g}A_t\right]-\tfrac{1}{2}k_{\omega\omega}A_{tt}$$
$$=-\varepsilon_2\frac{I_S\omega^2}{2kc^2}\left[1-\frac{1}{|A|^2/I_S}+\frac{\exp(-|A|^2/I_S)}{|A|^2/I_S}\right]A ,$$
$$(8)$$

where v_g is the group velocity, and we have taken into account that for the HE_{11} mode $\beta_0\approx\omega\sqrt{\varepsilon}/c=k$, k being the wave number. Note that from here onward a suffix stands for the partial derivative with respect to this unless stated otherwise.

In order to write Eq. (8) in dimensionless form, we introduce the following variables:

$$q=\frac{A}{\sqrt{I_S}},\xi=\left[\frac{\omega}{c}n_2 I_S\right]x,$$
$$\tau=\left[\frac{\omega}{c}\frac{n_2 I_S}{(-k_{\omega\omega})}\right]^{1/2}\left[t-\frac{x}{v_g}\right] ,$$
$$(9)$$

where we have assumed that we are working in the anomalous dispersion region in which $(-k_{\omega\omega})>0$. As a result Eq. (8) can be written as [28,29]

$$iq_\xi+\tfrac{1}{2}q_{\tau\tau}+q\left[1-\frac{1}{|q|^2}+\frac{\exp(-|q|^2)}{|q|^2}\right]=0 .\qquad (10)$$

This is the basic evolution equation describing pulse dynamics in our model in the absence of dissipation, which can be accounted for easily and which we shall deal with below.

For convenience let us also write down the model equation for the case of Δn_{NL} given by Eq. (3) in dimensionless form, taking into account transformations (9). It has the following form [22]:

$$iq_\xi+\tfrac{1}{2}q_{\tau\tau}+q\frac{|q|^2}{1+|q|^2}=0 .\qquad (11)$$

Note that Eqs. (10) and (11) differ not only in the functional form of nonlinearity but also in the fact that while Eq. (11) is an unaveraged model Eq. (10) has been derived by performing averaging over the fiber cross section. Averaging is desirable, since the transverse distribution of the electric field of the mode is not uniform over the fiber cross section.

The model described by Eq. (10) will be referred to as the K model, while the one described by Eq. (11) as the fractional model (f model). In what follows we shall determine the soliton solutions in both these models and compare their properties.

III. SOLITON SOLUTIONS (LOSSLESS CASE)

We look for the fundamental (i.e., $N=1$ in terms of the inverse scattering method) bright soliton solutions to Eqs. (10) and (11) satisfying

$$\lim_{\tau\to\pm\infty}q(\xi,\tau)=\lim_{\tau\to\pm\infty}q_\tau(\xi,\tau)=0\qquad (12)$$

and the condition of stationarity in ξ. Following Hasegawa [27], we put

$$q(\xi,\tau)=[\Psi(\xi,\tau)]^{1/2}\exp[i\Phi(\xi,\tau)] .\qquad (13)$$

Then from (10) and (13) we obtain

$$\frac{1}{\Psi}\Psi_\xi+\Phi_{\tau\tau}+\frac{1}{\Psi}\Psi_\tau\Phi_\tau=0 ,\qquad (14)$$

$$-\Phi_\xi+\frac{1}{4\Psi}\Psi_{\tau\tau}-\frac{1}{8\Psi^2}(\Psi_\tau)^2-\tfrac{1}{2}(\Phi_\tau)^2$$
$$+\left[1-\frac{1}{\Psi}+\frac{\exp(-\Psi)}{\Psi}\right]=0 ,\qquad (15)$$

where, according to Eq. (12), the amplitude Ψ satisfies

$$\lim_{\tau\to\pm\infty}\Psi(\xi,\tau)=\lim_{\tau\to\pm\infty}\Psi_\tau(\xi,\tau)=0 .\qquad (16)$$

As usual the condition of stationarity in ξ gives $\Psi_\xi=0$, and hence from (14) we obtain

$$\Psi(\tau)\Phi_\tau=c(\xi) .\qquad (17)$$

As is well known [27], the conditions of stationarity in ξ and localization in τ can be satisfied only if $c(\xi)=0$. As a result we obtain

$$\Phi=\beta\xi+\Phi_0 ,\qquad (18)$$

where $\Phi_0=\Phi|_{\xi=0}$, and β is a constant that represents the nonlinear addition to the propagation constant. Substituting for Φ from Eq. (18) into Eq. (15), we obtain

$$\frac{1}{4\Psi}\Psi''-\frac{1}{8\Psi^2}\Psi'^2-\left[\frac{1-\exp(-\Psi)}{\Psi}\right]+(1-\beta)=0 ,\qquad (19)$$

where the prime stands for the ordinary derivative with respect to τ. A similar treatment of Eq. (11) leads to the following results for the f model. The phase Φ is again given by Eq. (18), but Ψ satisfies the following differential equation:

$$\frac{1}{4\Psi}\Psi''-\frac{1}{8\Psi^2}\Psi'^2+\frac{\Psi}{1+\Psi}-\beta=0 .\qquad (20)$$

In order to determine the soliton solutions we must integrate Eqs. (19) and (20) numerically. For that we need appropriate values of β, since not for all β's but only for some particular values, for a given input amplitude Ψ_0, Eq. (19) or (20) will have bright soliton type solutions. If

we multiply Eq. (19) by Ψ' and use the boundary conditions (16), we obtain

$$\frac{1}{8}\left[\frac{d\Psi}{d\tau}\right]^2+(1-\beta)\Psi-Ein(\Psi)=0\ ,\tag{21}$$

where Ein is defined through the integral exponential function E_1 and Euler constant ζ as [31]

$$Ein\,(y)=E_1(y)+\ln(y)+\zeta\ .\tag{22}$$

Since we are looking for $N=1$ bright soliton solutions with a maximum $q_0=\sqrt{\Psi_0}$ at $\tau=0$, we arrive at

$$\beta=1-\frac{Ein(\Psi_0)}{\Psi_0}\ .\tag{23}$$

Similarly one can obtain β for the f model. It is given by

$$\beta=1-\frac{\ln(1+\Psi_0)}{\Psi_0}\ .\tag{24}$$

IV. NUMERICAL RESULTS

For a given value of Ψ_0 we determine the corresponding value of β and then numerically integrate Eqs. (19) and (20) to determine $\Psi(\tau)$, i.e., the soliton shape. The results of our study are depicted in Figs. 1–12. Note that in all our figures the solid line corresponds to the results of the K model, while the broken line represents those for the f model.

Figure 1 contains the soliton peak amplitude as a function of the dimensionless soliton energy

$$\mathcal{E}=I_0S\int_{-\infty}^{+\infty}|f(\tau)|^2d\tau\ ,\tag{25}$$

where $I_0=|q_0|^2$ is the dimensionless peak intensity of the soliton, S is the effective cross sectional area of the fiber, and $f(\tau)$ is the soliton shape function. Note that $S(K$ model)$/S(f$ model) $=2(r_0/a)^2\approx\frac{1}{2}$ in the Gaussian approximation [32], where r_0 is the distance at which the intensity drops by a factor of $1/e$, and a is the fiber core radius. In comparing solitons of equal energy we have to take this fact into account. Figure 2 contains the soliton width τ_0 as a function of the energy $\mathcal{E}$.

If we analyze these figures, we conclude that both models admit two-state soliton solutions in the sense that for a given set of fiber parameters there exist two solitons
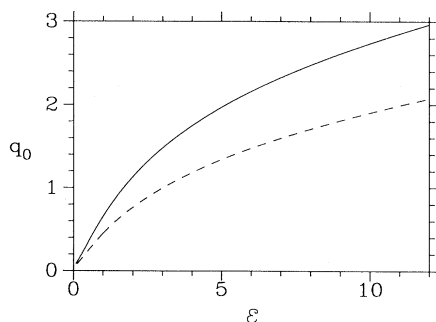

FIG. 1. Soliton pulse amplitude as a function of dimensionless energy $\mathcal{E}$. K model: solid curve; f model: dashed curve.
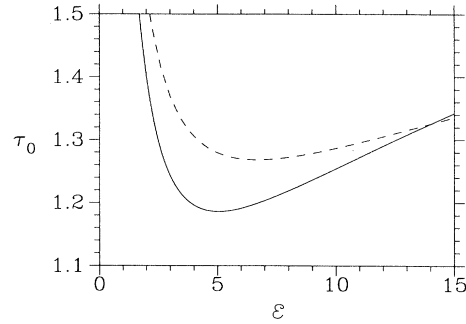

FIG. 2. Soliton width τ_0 as a function of dimensionless energy $\mathcal{E}$. K model: solid curve; f model: dashed curve.
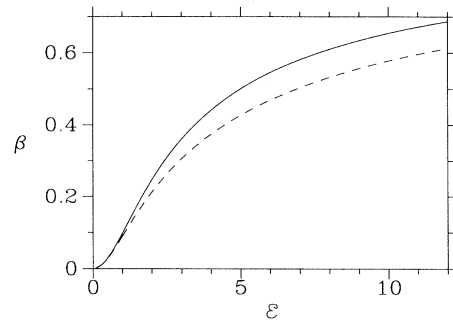

FIG. 3. Nonlinear propagation constant shift β as a function of dimensionless energy $\mathcal{E}$. K model: solid curve; f model: dashed curve.
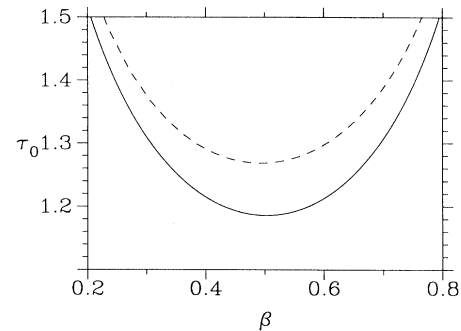

FIG. 4. Soliton width τ_0 as a function of the nonlinear propagation constant shift β. K model: solid curve; f model: dashed curve.
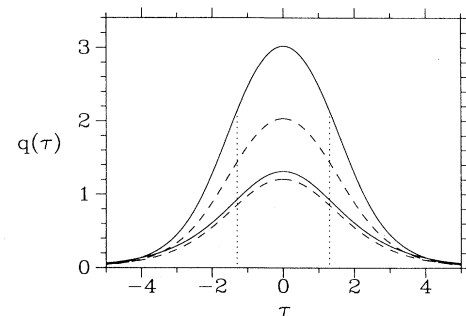

FIG. 5. Soliton shapes for $\tau_0=1.3$. K model: solid curve; f model: dashed curve. The vertical lines indicate the full width at half maximum intensity.
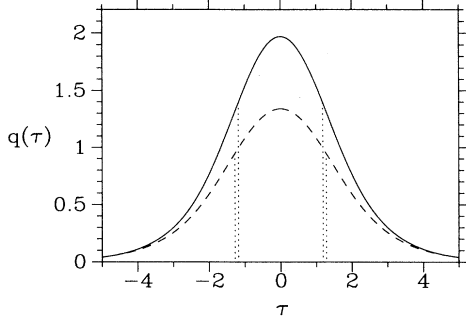
FIG. 6. Soliton shapes for energy $\mathscr{E}=5$. K model: solid curve; f model: dashed curve. The vertical lines indicate the full width at half maximum intensity.
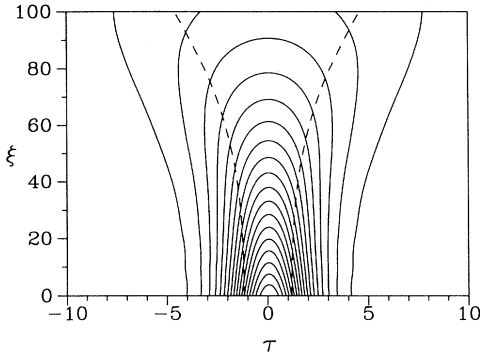

FIG. 7. Contour plot for $\mathscr{E}=5$ and $\Gamma=0.0138$ in the K model. The dashed line depicts the variation of the soliton width.
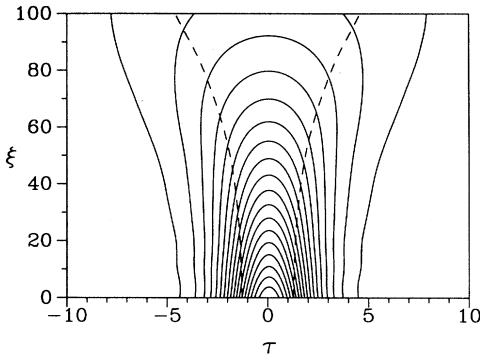

FIG. 8. Contour plot for $\mathscr{E}=5$ and $\Gamma=0.0138$ in the f model. The dashed line depicts the variation of the soliton width.
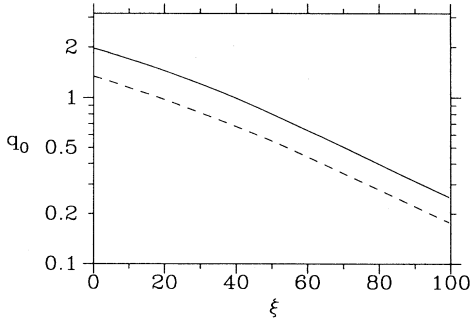

FIG. 9. Soliton peak amplitude q_0 as a function of propagation distance ξ for $\mathscr{E}=5$ and $\Gamma=0.0138$. K model: solid curve; f model: dashed curve.

with the same width but different energies and hence different peak powers and shapes. Figure 3, which has β as a function of soliton energy $\mathscr{E}$, shows that the solitons in these models are not bistable in the sense advocated by Kaplan [15,16], since $\mathscr{E}$ is not a double-valued but a monotonic function of β. However, as shown in Fig. 4, the soliton width is a double-valued function of β. For illustration the shapes of the two-state solitons in both the models for the same value of the pulse width ($\tau_0=1.3$) have been depicted in Fig. 5.

Further it is clear from Fig. 2 that the soliton width obtainable in both models is bounded from below: $\tau_0 \geq \tau_{0m}$, where τ_{0m} is the minimum pulse width. The smallest pulse width predicted by the K model is $\tau_{0m}=1.186$ for $\mathscr{E}=5.028$, and that by the f model is $\tau_{0m}=1.268$ for $\mathscr{E}=6.663$. Figure 2 also shows that for smaller values of $\mathscr{E}$ each τ_0 corresponds to a single value of energy, and hence the models have single soliton solutions. This is understandable, since for smaller values of power, expanding the nonlinear functions into series and retaining only the leading order term in the evolution equations in both the models, we recover the usual nonlinear Schrödinger equation which does not admit two-state solitons. Finally it is clear from Fig. 3 that solitons in both the models are stable under small perturbations, since the stability criterion $d\mathscr{E}/d\beta>0$ is satisfied in the whole range of β values.

V. SOLITON BEHAVIOR UNDER FIBER LOSS

The linear dissipation in a fiber can be accounted for by adding a dissipation term $-i\alpha A$ to the right-hand side of Eq. (8), where α is the phenomenological loss coefficient measured in decibels per kilometer. After the nondimensionalization given by Eq. (9), we obtain a dissipation term $-i\Gamma q$ on the right-hand side of Eq. (10), where

$$\Gamma=\frac{c\alpha}{\omega n_2 I_s} \qquad (26)$$

is the dimensionless loss coefficient. As a result, the pulse dynamics is governed by

$$iq_\xi+\tfrac{1}{2}q_{\tau\tau}+q\left[1-\frac{1}{|q|^2}+\frac{\exp(-|q|^2)}{|q|^2}\right]=-i\Gamma q$$
$$(K \text{ model}) , \qquad (27)$$

$$iq_\xi+\tfrac{1}{2}q_{\tau\tau}+q\frac{|q|^2}{1+|q|^2}=-i\Gamma q \quad (f \text{ model}) . \qquad (28)$$

We have numerically integrated Eqs. (27) and (28) using the symmetrized split-step Fourier method. As initial condition we chose the soliton solution of the lossless equation for a given soliton energy $\mathscr{E}$. The soliton evolution for $\Gamma=0.0138$, corresponding to a loss rate of 0.12 dB/km, and $\mathscr{E}=5$ is given as a contour plot in Fig. 7 for the K model and in Fig. 8 for the f model. Figure 9 contains the variation of the soliton amplitude with the distance of propagation, while Fig. 10 depicts the evolution of the pulse width as a function of ξ. From these figures
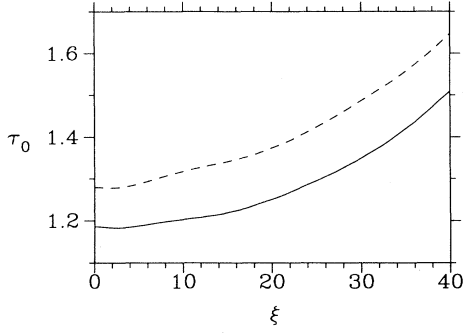
FIG. 10. Soliton width variation with the distance of propagation for $\mathscr{E}=5$ and $\Gamma=0.0138$. K model: solid curve; f model: dashed curve.

it is clear that initially the soliton width τ_0 increases slowly, showing that the soliton tries to preserve its soliton property. Subsequently, because of the considerable decrease in the soliton amplitude, dispersion takes over and the pulse width monotonically increases at a faster rate, as is visible from Fig. 10. All this is consistent with the results of soliton perturbation theory [21] for the nonlinear Schrödinger equation. The quantitative difference may be assigned to the strong saturating nonlinearity. It is also worth mentioning that for higher values of energy we see from the contour plots (Fig. 11 for the K model and Fig. 12 for the f model) that the pulse width initially decreases and then starts increasing, leading subsequently to pulse dispersion.

VI. COMPARISON OF RESULTS FOR THE TWO MODELS

It is easy to conclude from Figs. 1 and 2 that for a given value of energy $\mathscr{E}$ within the range investigated, the soliton in the K model is sharper, i.e., narrower with a smaller width, and has a higher peak power. Figure 6, in which we have plotted the soliton shapes with the same energy $\mathscr{E}=5.0$ in both models, clearly confirms this statement. It is also clear from Fig. 3 that for a given energy $\mathscr{E}$ the nonlinear propagation constant β or, equivalently, the self-phase modulation is higher in the K model. In turn, since β is a monotonically increasing function of the soliton peak intensity, a higher value of β
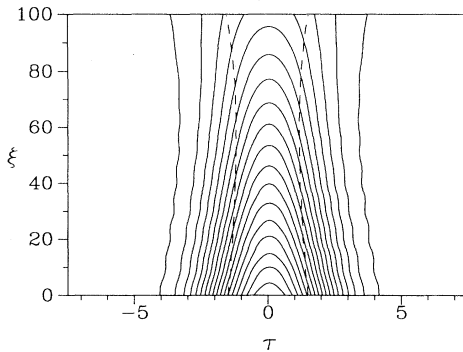

FIG. 11. Contour plot for $\mathscr{E}=25$ and $\Gamma=0.0138$ in the K model. The dashed line depicts the variation of the soliton width.
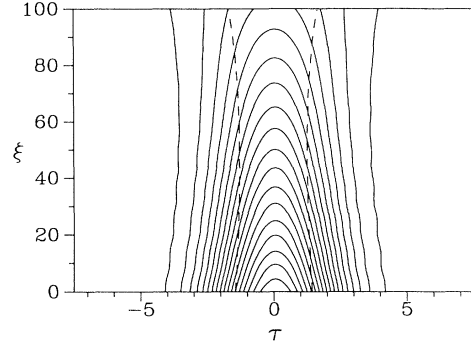

FIG. 12. Contour plot for $\mathscr{E}=25$ and $\Gamma=0.0138$ in the f model. The dashed line depicts the variation of the soliton width.

for a given energy clearly indicates a higher peak intensity and hence sharper characteristics of solitons in the K model. This property is pronounced in the region of pulse energy $2 \leq \mathscr{E} \leq 8$. From Figs. 1 and 2 it can be seen that the minimum soliton pulse width obtainable, in the relevant range of energy, is always less in the K model than in the f model. For example, τ_{0m} in the K model is approximately 7.2% less than its value in the f model for $\mathscr{E}=5$, while it is 9.2% less for $\mathscr{E}=2.5$. Also, for $1.186 \leq \tau_0 < 1.268$ there is no two-state soliton in the f model. Hence we can conclude that to achieve the same effectiveness in switching with sharper soliton characteristics, we need less energy in the K model compared to the f model.

Finally, we see from Fig. 10 that in the lossy case a soliton of the same energy $\mathscr{E}$ propagates a larger distance in the K model compared to the corresponding soliton in the f model before undergoing the same amount of broadening. Hence the solitons in the K model behave in a more robust way under the influence of fiber loss than the solitons in the f model. By this we mean the following. Suppose in a practical system that there is an upper limit (say τ_l) of tolerance on the soliton width related to detection or stability or switching, etc. Then Fig. 10 shows that the solitons of the K model propagate for a larger distance compared to the solitons in the f model before the soliton width reaches the critical value τ_l.

VII. CONCLUSION

We have obtained and studied the properties of the fundamental bright solitons numerically in the K model, Eqs. (10) and (27), as well as in the f model, Eqs. (11) and (28). Our results show that both these models do not contain bistable soliton solutions in the sense advocated by Kaplan [15], but they do admit two-state soliton solutions which will be useful for studies related to switching. Further, our results clearly show that if we compare solitons, with the same value of energy in the given models, then the solitons in the K model are sharper, i.e., narrower and taller, and that they are more robust under the influence of fiber loss. Also, for a given pulse width the energy needed for the generation of two-state solitons is less, and the range of soliton widths for which two-state solitons exist is larger in the K model than the f model.

[1] A. Hasegawa and F. Tappert, Appl. Phys. Lett. **23**, 142 (1973); **23**, 171 (1973).

[2] L. F. Mollenauer, J. P. Gordon, and N. N. Islam, IEEE J. Quantum Electron. **QE-22**, 157 (1986).

[3] L. F. Mollenauer, R. H. Stolen, and J. P. Gordon, Phys. Rev. Lett. **45**, 1099 (1980).

[4] K. J. Blow and N. J. Doran, IEE Proc. J. **134**, 137 (1987).

[5] Ajit Kumar, Phys. Rep. **187**, 63 (1990).

[6] H. Kubota and N. Nakazawa, IEEE J. Quantum Electron. **QE-26**, 692 (1990).

[7] A. Hasegawa and Y. Kodama, Phys. Rev. Lett. **66**, 161 (1991).

[8] Y. Kodama and A. Hasegawa, Opt. Lett. **17**, 81 (1992).

[9] G. P. Agrawal, *Nonlinear Fiber Optics,* 2nd ed. (Academic, San Diego, 1995).

[10] A. Mecozzi, J. D. Moores, H. A. Haus, and Y. Lai, Opt. Lett. **16**, 1841 (1991).

[11] M. N. Islam, Opt. Lett. **14**, 457 (1989).

[12] N. J. Doran and D. Wood, J. Opt. Soc. Am. B **4**, 1843 (1989).

[13] R. H. Enns and S. S. Rangnekar, IEEE J. Quantum Electron. **QE-23**, 1199 (1987).

[14] R. H. Enns, D. E. Edmundson, S. S. Rangnekar, and A. E. Kaplan, Opt. Quantum Electron. **24**, S1295 (1992).

[15] A. E. Kaplan, Phys. Rev. Lett. **55**, 1219 (1985).

[16] A. E. Kaplan, IEEE J. Quantum Electron. **QE-21**, 1538 (1985).

[17] R. H. Enns and S. S. Rangnekar, Phys. Rev. Lett. **57**, 778 (1986).

[18] R. H. Enns and S. Rangnekar, Phys. Rev. A **45**, 3354 (1992).

[19] D. E. Edmundson and R. H. Enns, Opt. Lett. **17**, 586 (1992).

[20] P. Roussignol, D. Ricard, J. Lukasik, and C. Flytzantis, J. Opt. Soc. Am. B **4**, 5 (1987).

[21] D. J. Kaup and A. C. Newell, Proc. R. Soc. London Ser. A **361**, 413 (1978).

[22] S. Gatz and J. Herrmann, J. Opt. Soc. Am. B **8**, 2296 (1991).

[23] M. L. Lyra and A. S. Gouveia-Neto, Opt. Commun. **108**, 117 (1994).

[24] Ajit Kumar, in *Proceedings of the SPIE Conference on Emerging Optoelectronic Technologies (Bangalore, December, 1991),* edited by A. Selvarajan *et al.* (Tata McGraw-Hill, Bombay, 1992), p. 252.

[25] C. DeAngelis, IEEE J. Quantum Electron. **QE-30**, 818 (1994).

[26] H. Hatami-Hanza, P. L. Chu, and G. D. Peng, Opt. Quantum Electron. **27**, 193 (1994).

[27] A. Hasegawa, *Optical Solitons in Fibers* (Springer, Heidelberg, 1989).

[28] Ajit Kumar, J. Mod. Opt. **38**, 11 (1991).

[29] Ajit Kumar, Opt. Commun. **84**, 346 (1991).

[30] J.-L. Coutaz and M. Kull, J. Opt. Soc. Am. B **8**, 95 (1991).

[31] *Handbook of Mathematical Functions,* edited by A. Abramowitz and I. Stegun (Dover, New York, 1972), Chap. 5, Sec. 5.1.53.

[32] E. P. Ippen, in *Laser Applications to Optics and Spectroscopy,* edited by S. F. Jacobs *et al.* (Addison-Wesley, Reading, MA, 1975), p. 220.